



Crystal structure and characterization of a new copper(II) chloride dimer with methyl(pyridin-2-ylmethylidene)amine

Olga Yu. Vassilyeva,^{a*} Elena A. Buvaylo,^a Vladimir N. Kozozay,^a Andrii K. Melnyk^b and Brian W. Skelton^c

Received 15 April 2020
Accepted 29 April 2020

Edited by S. Parkin, University of Kentucky, USA

Keywords: crystal structure; Cu^{II} dimer; Schiff base ligand; 2-pyridinecarbaldehyde; methylamine.

CCDC reference: 1981381

Supporting information: this article has supporting information at journals.iucr.org/e

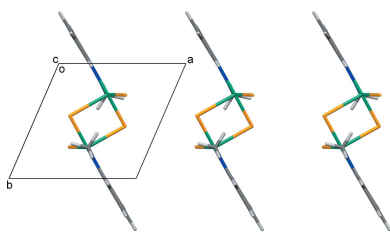
^aDepartment of Chemistry, Taras Shevchenko National University of Kyiv, 64/13 Volodymyrska str., Kyiv 01601, Ukraine, ^bInstitute for Sorption and Problems of Endoecology, The National Academy of Sciences of Ukraine, 13 General Naumova str., Kyiv 03164, Ukraine, and ^cSchool of Molecular Sciences, M310, University of Western Australia, Perth, WA 6009, Australia. *Correspondence e-mail: vassilyeva@univ.kiev.ua

The new copper(II) complex, namely, di- μ -chlorido-bis{chlorido[methyl(pyridin-2-ylmethylidene)amine- κ^2N,N']copper(II)}, [Cu₂Cl₄(C₇H₈N₂)₂], (I), with the ligand 2-pyridylmethyl-*N*-methylimine (*L*, a product of Schiff base condensation between methylamine and 2-pyridinecarbaldehyde) is built of discrete centrosymmetric dimers. The coordination about the Cu^{II} ion can be described as distorted square pyramidal. The base of the pyramid consists of two nitrogen atoms from the bidentate chelate *L* [Cu–N = 2.0241 (9), 2.0374 (8) Å] and two chlorine atoms [Cu–Cl = 2.2500 (3), 2.2835 (3) Å]. The apical position is occupied by another Cl atom with the apical bond being significantly elongated at 2.6112 (3) Å. The *trans* angles of the base are 155.16 (3) and 173.79 (2)°. The Cu···Cu separation in the dimer is 3.4346 (3) Å. In the crystal structure, the loosely packed dimers are arranged in stacks propagating along the *a* axis. The X-band polycrystalline 77 K EPR spectrum of (I) demonstrates a typical axial pattern characteristic of mononuclear Cu^{II} complexes. Compound (I) is redox active and shows a cyclic voltammetric response with $E_{1/2} = -0.037$ V versus silver–silver chloride electrode (SSCE) assignable to the reduction peak of Cu^{II}/Cu^I in methanol as solvent.

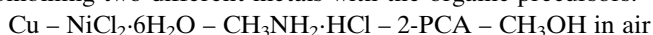
1. Chemical context

The crystal structure of the title compound was determined as part of our ongoing research focused on the design and synthesis of the organic–inorganic halometallates with substituted imidazo[1,5-*a*]pyridinium cations. The first cation in the series, 2-methyl-3-(pyridin-2-yl)imidazo[1,5-*a*]pyridinium, was obtained by the replacement of a conventional aqueous solution of methylamine with its solid hydrochloride salt in the reaction with 2-pyridinecarbaldehyde (2-PCA) in methanol (Buvaylo *et al.*, 2015). The cation is a result of the acid-catalysed oxidative condensation–cyclization between two molecules of 2-PCA and one molecule of CH₃NH₂ with the acid added as an adduct of the amine. The prepared *in situ* organic cation forms a halometallate salt in the subsequent interaction with divalent metal halides (*M* = Mn, Co, Zn, Cd) or can be isolated in salt form with Cl[−]/NO₃[−] anions (Buvaylo *et al.*, 2015; Vassilyeva *et al.*, 2019*a,b*, 2020).

The burgeoning research in the field of organic–inorganic halometallate-based hybrids in search of new applications (Wheaton *et al.*, 2018; Yangui *et al.*, 2019; Szklarz *et al.*, 2020) prompted us to extend the developed reaction to the possible

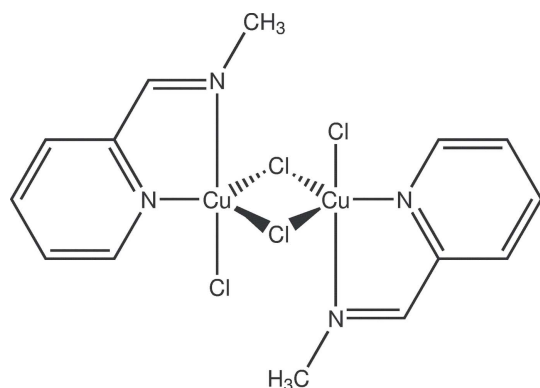


preparation of a mixed-metal hybrid halometallate by combining two different metals with the organic precursors:



Adhering to the *direct synthesis* approach (Kokozay *et al.*, 2018), one of the metals was introduced in a zerovalent state. Our earlier studies showed that a metal powder was oxidized in solution to form a coordination compound in the presence of a proton-donating agent and dioxygen from the air, this being reduced to give H_2O .

Such a complication of the reaction system had an adverse effect, precluding formation of the desired heterocycle with the imidazo[1,5-*a*]pyridinium skeleton but afforded the Schiff base 2-pyridylmethyl-*N*-methylimine (*L*) instead. The latter is a pale-yellow liquid usually accessible by a straightforward interaction of 2-PCA with a 40% aqueous solution of methylamine (Schulz *et al.*, 2009). In the present work, the imine *L* was isolated as the copper(II) complex $[\text{CuLCl}_2]_2$, (I), the dimeric structure of which has been established by X-ray crystallography. The title compound was characterized by elemental analysis, IR and EPR spectroscopy as well as cyclic voltammetry.



2. Structural commentary

The title complex crystallizes in the triclinic space group, $P\bar{1}$; the dimeric molecule is situated on a crystallographic inversion centre. The coordination about the Cu atom can be

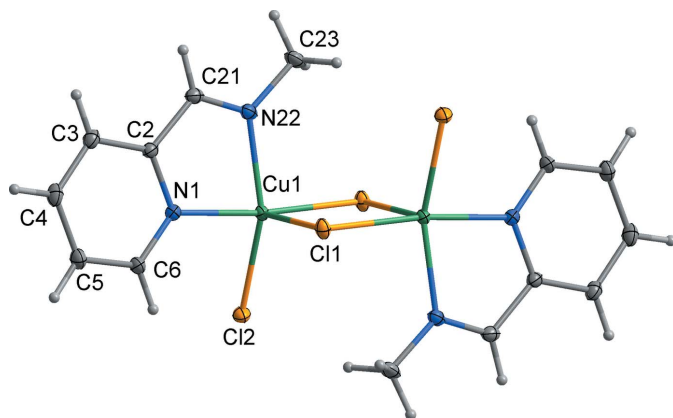


Figure 1
Molecular structure and principal labelling of $[\text{CuLCl}_2]_2$ (I) with ellipsoids at the 50% probability level.

Table 1
Selected geometric parameters (\AA , $^\circ$).

Cu1—N1	2.0241 (9)	Cu1—Cl1 ⁱ	2.2835 (3)
Cu1—N22	2.0374 (8)	Cu1—Cl1	2.6112 (3)
Cu1—Cl2	2.2500 (3)		
N1—Cu1—N22	80.20 (3)	N1—Cu1—Cl1	88.81 (3)
N1—Cu1—Cl2	92.29 (2)	N22—Cu1—Cl1	94.79 (3)
N22—Cu1—Cl2	155.16 (3)	Cl2—Cu1—Cl1	108.803 (10)
N1—Cu1—Cl1 ⁱ	173.79 (2)	Cl1 ⁱ —Cu1—Cl1	91.137 (10)
N22—Cu1—Cl1 ⁱ	93.61 (3)	Cu1 ⁱ —Cl1—Cu1	88.864 (11)
Cl2—Cu1—Cl1 ⁱ	93.600 (11)		

Symmetry code: (i) $-x + 1, -y + 1, -z + 1$.

described as distorted square pyramidal. The angular structural index parameter, $\tau = (\beta - \alpha)/60$, evaluated from the two largest angles ($\alpha < \beta$) in the five-coordinated geometry, which has ideal values of 1 for an equilateral bipyramid and 0 for a square pyramid, is equal to 0.31 (Table 1). The base of the pyramid consists of the two nitrogen atoms, N1, N22 from the bidentate chelate ligand *L* and the two chlorine atoms, Cl2 and the centrosymmetrically related Cl1 of the dimer (Fig. 1). Bond parameters are unexceptional (Table 1). The apical position is occupied by the Cl1 atom with the apical bond being significantly elongated at 2.6112 (3) \AA compared to the Cu1—Cl1ⁱ bond length of 2.2835 (3) \AA [symmetry code: (i) $1 - x, 1 - y, 1 - z$]. The *trans* angles of the base are N22—Cu1—Cl2 = 155.16 (3) $^\circ$ and N1—Cu1—Cl1ⁱ = 173.79 (2) $^\circ$. The *cis* angles at the copper atom vary from 80.20 (3) to 108.803 (10) $^\circ$. The Cu \cdots Cuⁱ separation in the dimer is 3.4346 (3) \AA .

3. Supramolecular features

In the crystal structure, the dimers are arranged in stacks propagating along the *a*-axis direction and demonstrate loose packing (Fig. 2). The shortest distance between the Cl atoms of adjacent molecules is 4.4204 (5) \AA for Cl2 \cdots Cl2ⁱⁱ [symmetry code: (ii) $1 - x, 2 - y, 2 - z$] and the minimum separation between Cu atoms inside the stack is as long as 7.1550 (5) \AA for Cu1 \cdots Cu1ⁱⁱⁱ [symmetry code: (iii) $-x, 1 - y, 1 - z$]. The neighbouring pyridyl rings along the stack are

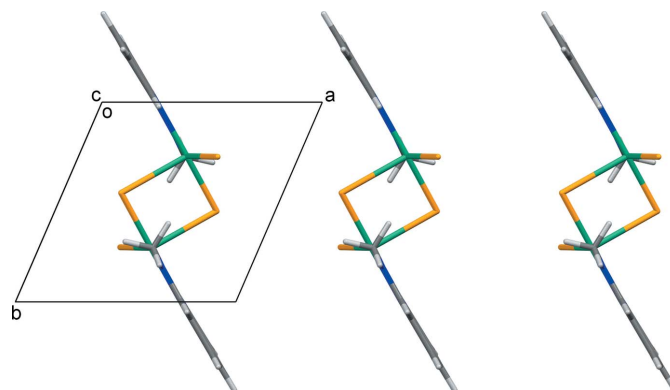


Figure 2
Fragment of crystal packing of $[\text{CuLCl}_2]_2$ (I) viewed along the *c*-axis direction.

coplanar, with the ring centroid distance being equal to the a -axis length [7.7054 (5) Å], which is too great for π -overlap.

4. Database survey

A survey of the Cambridge Structural Database (CSD, Version 5.40, October 2019; Groom *et al.*, 2016) reveals that crystal structures containing L as a ligand comprise seven examples of divalent Mn, Ni, Zn and Pd as well as tetravalent Sn compounds. Among these metal complexes, the ligand demonstrates the same coordination mode as in compound (I) both in monomeric Ni [CSD refcode ADIQOV (Bai *et al.*, 2012); NEKYOT (Pioquinto-Mendoza *et al.*, 2013)], Zn (BULSUX; Schulz *et al.*, 2009), Pd (NEKYUZ; Pioquinto-Mendoza *et al.*, 2013) and Sn coordination compounds (NELKAS and NELKEW; Guzmán-Percástegui *et al.*, 2013) and Zn (BULSUX; Schulz *et al.*, 2009) and Mn (VECDJ; Bai *et al.*, 2006) dimers. Out of all the L complexes, only the nickel ones accommodate two ligands in the coordination sphere of the metal ion.

5. IR and EPR spectroscopy measurements

A broad band centred at about 3440 cm^{-1} in the IR spectrum of (I) could be due to adsorbed water molecules (see supporting information). Several bands arising above and below 3000 cm^{-1} are assigned to aromatic $=\text{CH}$ and alkyl $-\text{CH}$ stretching, respectively. The characteristic $\nu(\text{C}=\text{N})$ absorption of the Schiff base, which appears at 1652 cm^{-1} as a sharp and rather intense band in the IR spectrum of L (Schulz *et al.*, 2009), is detected at 1648 cm^{-1} in the spectrum of (I). A number of sharp and intense absorptions are observed in the aromatic ring stretching ($1600\text{--}1400\text{ cm}^{-1}$) and C–H out-of-plane bending regions ($800\text{--}700\text{ cm}^{-1}$).

The X-band polycrystalline EPR spectra of (I) (Fig. 3) show a typical axial pattern characteristic for the mononuclear Cu^{II} complexes with no visible hyperfine structure. The spectra are almost temperature independent with a subtle change of their shapes seen between 293 and 77 K. The axial symmetry characteristics of (I), $g_{\parallel} = 2.26$ and $g_{\perp} = 2.06$, with a $g_{\parallel} > g_{\perp} > 2.02$ relation confirm a square-pyramidal coordination

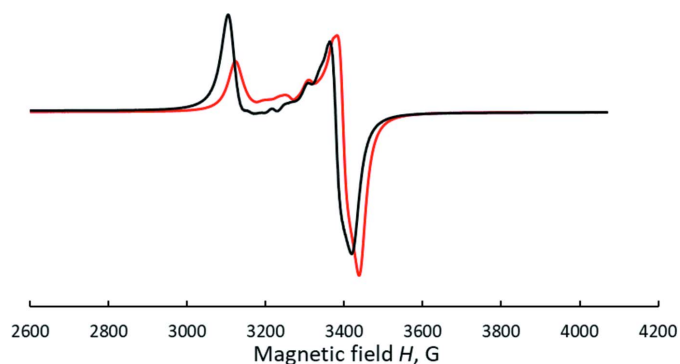


Figure 3
X-band EPR spectra of $[\text{CuLCl}_2]_2$ (I) in the solid state at 293 (red) and 77 K (black).

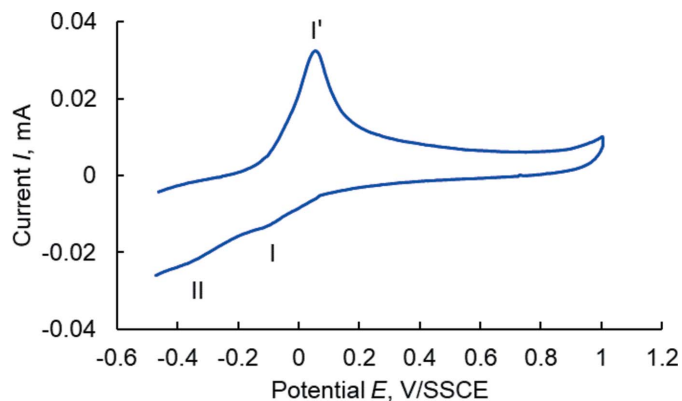


Figure 4
Cyclic voltammogram of $[\text{CuLCl}_2]_2$ (I), 0.1 mM in methanol mixed with 0.1 M acetate buffer (pH 4) and NaClO_4 (70:28:2) as supporting electrolyte at a glassy carbon electrode and Ag/AgCl as reference electrode (scan rate: 100 mV s^{-1} ; $T = 298\text{ K}$).

geometry for the metal centre suggested by the structural data. The additional low intensity lines at $g_{\text{eff}} = 2.18, 2.16$ and 2.12 may indicate exchange interactions between copper(II) ions in the dimer that are probably very weak.

6. Cyclic voltammetry

Compound (I) is redox active and shows a cyclic voltammetric response in the potential range of $-0.12\text{--}0.047\text{ V}$ ($E_{1/2} = -0.037\text{ V vs SSCE}$), which is assignable to the reduction peak of $\text{Cu}^{\text{II}}/\text{Cu}^{\text{I}}$ (Fig. 4). The complex exhibits quasi-reversible behaviour as indicated by the non-equivalent current intensity of cathodic and anodic peaks ($i_c/i_a = 0.422$) and a large separation between them (167 mV) (Crutchley *et al.*, 1990). Since Cu^{I} prefers to be four-coordinate, the irreversibility of the $\text{Cu}^{\text{II}}/\text{Cu}^{\text{I}}$ couple may be due to the dissociation of the dimers in solution. Reduction of copper(I) to copper(0) is associated with the irreversible peak at -0.36 V vs SSCE . The latter process causes removal of the metal centre from the complex molecule. The resulting free ligand undergoes reduction at about -0.8 V , which is superimposed with the reduction peak of the solvent, as is evident from the comparison between the cyclic voltammograms of (I) and supporting electrolyte methanol solutions.

7. Synthesis and crystallization

2-PCA (0.19 ml, 2 mmol) was magnetically stirred with $\text{CH}_3\text{NH}_2\cdot\text{HCl}$ (0.27 g, 4 mmol) in 20 ml methanol in a 50 ml Erlenmeyer flask at room temperature (r.t.) for an hour. Dry $\text{NiCl}_2\cdot 6\text{H}_2\text{O}$ (0.23 g, 1 mmol) and Cu powder (0.06 g, 1.0 mmol) were added to the resulting yellow solution of the preformed Schiff base. The mixture immediately turned green and was magnetically stirred at 323 K in open air to achieve dissolution of the metallic copper (4 h). The resulting solution was filtered and left to evaporate at r.t. Green plate-like crystals of (I) suitable for X-ray analysis deposited over two days. They were filtered off, washed with diethyl ether and

finally dried in air. Yield (based on Cu): 71%. Analysis calculated for $C_{14}H_{16}Cl_4Cu_2N_4$ (509.19): C 33.02, H 3.17, N 11.00%. Found: C 33.29, H 3.30, N 10.74%. IR (ν , cm^{-1} , KBr): 3438 br , 3092, 3068, 3022, 2992, 2922, 1648, 1598 vs , 1568, 1474, 1434, 1364, 1300 s , 1272, 1224, 1156 s , 1108, 1050, 1024 vs , 980, 946, 882, 782 vs , 646, 514, 476, 420.

8. Refinement

Crystal data, data collection and structure refinement details are summarized in Table 2. Anisotropic displacement parameters were employed for the non-hydrogen atoms. All hydrogen atoms were added at calculated positions and refined by use of a riding model with isotropic displacement parameters based on those of the parent atom (C–H = 0.95 Å, $U_{iso}(H) = 1.2U_{eq}C$ for CH, C–H = 0.98 Å, $U_{iso}(H) = 1.5U_{eq}C$ for CH₃).

Funding information

Funding for this research was provided by: Ministry of Education and Science of Ukraine (project No. 19BF037-05).

References

- Bai, S. Q., Fang, C. J., He, Z., Gao, E. Q., Yan, C. H. & Hor, T. A. (2012). *Dalton Trans.* **41**, 13379–13387.
- Bai, S. Q., Gao, E. Q., He, Z., Fang, C. J., Yue, Y. F. & Yan, C. H. (2006). *Eur. J. Inorg. Chem.* **2006**, 407–415.
- Brandenburg, K. (1999). *DIAMOND*. Crystal Impact GbR, Bonn, Germany.
- Buvaylo, E. A., Kokozay, V. N., Linnik, R. P., Vassilyeva, O. Y. & Skelton, B. W. (2015). *Dalton Trans.* **44**, 13735–13744.
- Crutchley, R. J., Hynes, R. & Gabe, E. J. (1990). *Inorg. Chem.* **29**, 4921–4928.
- Farrugia, L. J. (2012). *J. Appl. Cryst.* **45**, 849–854.
- Groom, C. R., Bruno, I. J., Lightfoot, M. P. & Ward, S. C. (2016). *Acta Cryst.* **B72**, 171–179.
- Guzmán-Percástegui, E., Reyes-Mata, C. A., Martínez-Otero, D., Andrade-López, N. & Alvarado-Rodríguez, J. G. (2013). *Polyhedron*, **50**, 418–424.
- Kokozay, V. N., Vassilyeva, O. Y. & Makhankova, V. G. (2018). *Direct Synthesis of Metal Complexes*, edited by B. Kharisov, pp. 183–237. Amsterdam: Elsevier.
- Macrae, C. F., Sovago, I., Cottrell, S. J., Galek, P. T. A., McCabe, P., Pidcock, E., Platings, M., Shields, G. P., Stevens, J. S., Towler, M. & Wood, P. A. (2020). *J. Appl. Cryst.* **53**, 226–235.
- Pioquinto-Mendoza, J. R., Martínez-Otero, D., Andrade-López, N., Alvarado-Rodríguez, J. G., Salazar-Pereda, V., Sánchez-Cabrera, G. & Zuno-Cruz, F. J. (2013). *Polyhedron*, **50**, 289–296.

Table 2

Experimental details.

Crystal data	
Chemical formula	[Cu ₂ Cl ₄ (C ₇ H ₈ N ₂) ₂]
M_r	509.19
Crystal system, space group	Triclinic, $P\bar{1}$
Temperature (K)	100
a, b, c (Å)	7.7054 (5), 7.7240 (5), 8.5606 (5)
α, β, γ (°)	103.659 (5), 98.803 (5), 110.273 (5)
V (Å ³)	448.74 (5)
Z	1
Radiation type	Mo $K\alpha$
μ (mm ⁻¹)	2.97
Crystal size (mm)	0.56 × 0.41 × 0.16
Data collection	
Diffractometer	Oxford Diffraction Gemini diffractometer
Absorption correction	Analytical (<i>CrysAlis PRO</i> ; Rigaku OD, 2016)
T_{min}, T_{max}	0.367, 0.669
No. of measured, independent and observed [$I > 2\sigma(I)$] reflections	13153, 4238, 3866
R_{int}	0.024
$(\sin \theta/\lambda)_{max}$ (Å ⁻¹)	0.827
Refinement	
$R[F^2 > 2\sigma(F^2)], wR(F^2), S$	0.021, 0.054, 1.08
No. of reflections	4238
No. of parameters	111
H-atom treatment	H-atom parameters constrained
$\Delta\rho_{max}, \Delta\rho_{min}$ (e Å ⁻³)	0.68, -0.52

Computer programs: *CrysAlis PRO* (Rigaku OD, 2016), *SHELXT* (Sheldrick, 2015a), *SHELXL2017* (Sheldrick, 2015b), *DIAMOND* (Brandenburg, 1999), *Mercury* (Macrae, 2020) and *WinGX* (Farrugia, 2012).

- Rigaku OD (2016). *CrysAlis PRO*. Rigaku Oxford Diffraction Ltd, Yarnton, England.
- Schulz, M., Klopffleisch, M., Görls, H., Kahnes, M. & Westerhausen, M. (2009). *Inorg. Chim. Acta*, **362**, 4706–4712.
- Sheldrick, G. M. (2015a). *Acta Cryst.* **A71**, 3–8.
- Sheldrick, G. M. (2015b). *Acta Cryst.* **C71**, 3–8.
- Szklarz, P., Jakubas, R., Gągor, A., Bator, G., Cichos, J. & Karbowski, M. (2020). *Inorg. Chem. Front.* **7**, 1780–1789.
- Vassilyeva, O. Y., Buvaylo, E. A., Kokozay, V. N., Petrusenko, S. R., Melnyk, A. K. & Skelton, B. W. (2020). *Acta Cryst.* **E76**, 309–313.
- Vassilyeva, O. Y., Buvaylo, E. A., Kokozay, V. N., Skelton, B. W. & Sobolev, A. N. (2019b). *Acta Cryst.* **E75**, 1209–1214.
- Vassilyeva, O. Yu., Buvaylo, E. A., Kokozay, V. N., Skelton, B. W., Rajnáč, C., Titiš, Y. & Boča, R. (2019a). *Dalton Trans.* **48**, 11278–11284.
- Wheaton, A. M., Streep, M. E., Ohlhaber, C. M., Nicholas, A. D., Barnes, F. H., Patterson, H. H. & Pike, R. D. (2018). *ACS Omega*, **3**, 15281–15292.
- Yangui, A., Rocanova, R., McWhorter, T. M., Wu, Y., Du, M. H. & Saparov, B. (2019). *Chem. Mater.* **31**, 2983–2991.

supporting information

Acta Cryst. (2020). E76, 790-793 [https://doi.org/10.1107/S2056989020005903]

Crystal structure and characterization of a new copper(II) chloride dimer with methyl(pyridin-2-ylmethylidene)amine

Olga Yu. Vassilyeva, Elena A. Buvaylo, Vladimir N. Kozozay, Andrii K. Melnyk and Brian W. Skelton

Computing details

Data collection: *CrysAlis PRO* (Rigaku OD, 2016); cell refinement: *CrysAlis PRO* (Rigaku OD, 2016); data reduction: *CrysAlis PRO* (Rigaku OD, 2016); program(s) used to solve structure: SHELXT (Sheldrick, 2015a); program(s) used to refine structure: *SHELXL2017* (Sheldrick, 2015b); molecular graphics: *DIAMOND* (Brandenburg, 1999), *Mercury* (Macrae, 2020); software used to prepare material for publication: *WinGX* (Farrugia, 2012).

Di- μ -chlorido-bis[chlorido[methyl(pyridin-2-ylmethylidene)amine- κ^2N,N']copper(II)]

Crystal data

[Cu₂Cl₄(C₇H₈N₂)₂]

$M_r = 509.19$

Triclinic, *P*1

Hall symbol: -P 1

$a = 7.7054$ (5) Å

$b = 7.7240$ (5) Å

$c = 8.5606$ (5) Å

$\alpha = 103.659$ (5)°

$\beta = 98.803$ (5)°

$\gamma = 110.273$ (5)°

$V = 448.74$ (5) Å³

$Z = 1$

$F(000) = 254$

$D_x = 1.884$ Mg m⁻³

Mo $K\alpha$ radiation, $\lambda = 0.71073$ Å

Cell parameters from 7922 reflections

$\theta = 4.0$ – 37.5 °

$\mu = 2.97$ mm⁻¹

$T = 100$ K

Plate, green

$0.56 \times 0.41 \times 0.16$ mm

Data collection

Oxford Diffraction Gemini
diffractometer

Graphite monochromator

Detector resolution: 10.4738 pixels mm⁻¹

ω scans

Absorption correction: analytical

(*CrysAlis Pro*; Rigaku OD, 2016)

$T_{\min} = 0.367$, $T_{\max} = 0.669$

13153 measured reflections

4238 independent reflections

3866 reflections with $I > 2\sigma(I)$

$R_{\text{int}} = 0.024$

$\theta_{\max} = 36.0$ °, $\theta_{\min} = 4.2$ °

$h = -12 \rightarrow 12$

$k = -12 \rightarrow 12$

$l = -14 \rightarrow 14$

Refinement

Refinement on F^2

Least-squares matrix: full

$R[F^2 > 2\sigma(F^2)] = 0.021$

$wR(F^2) = 0.054$

$S = 1.08$

4238 reflections

111 parameters

0 restraints

Hydrogen site location: inferred from
neighbouring sites

H-atom parameters constrained

$$w = 1/[\sigma^2(F_o^2) + (0.0232P)^2 + 0.1399P]$$

$$\text{where } P = (F_o^2 + 2F_c^2)/3$$

$$(\Delta/\sigma)_{\max} = 0.002$$

$$\Delta\rho_{\max} = 0.68 \text{ e } \text{\AA}^{-3}$$

$$\Delta\rho_{\min} = -0.52 \text{ e } \text{\AA}^{-3}$$

Extinction correction: SHELXL-2017/1

(Sheldrick 2015b),

$$F_c^* = kFc[1 + 0.001xFc^2\lambda^3/\sin(2\theta)]^{-1/4}$$

Extinction coefficient: 0.018 (2)

Special details

Geometry. All esds (except the esd in the dihedral angle between two l.s. planes) are estimated using the full covariance matrix. The cell esds are taken into account individually in the estimation of esds in distances, angles and torsion angles; correlations between esds in cell parameters are only used when they are defined by crystal symmetry. An approximate (isotropic) treatment of cell esds is used for estimating esds involving l.s. planes.

Refinement. One low theta reflection was omitted from the refinement.

Fractional atomic coordinates and isotropic or equivalent isotropic displacement parameters (\AA^2)

	x	y	z	$U_{\text{iso}}^*/U_{\text{eq}}$
Cu1	0.50923 (2)	0.72999 (2)	0.57914 (2)	0.01020 (4)
Cl1	0.73459 (3)	0.54548 (3)	0.59992 (3)	0.01344 (5)
Cl2	0.36774 (3)	0.72631 (3)	0.79030 (3)	0.01500 (5)
N1	0.73406 (12)	0.98020 (12)	0.71584 (10)	0.01113 (13)
C2	0.82713 (14)	1.08198 (14)	0.62321 (12)	0.01197 (15)
C21	0.74454 (15)	0.99108 (15)	0.44328 (12)	0.01362 (16)
H21	0.797176	1.050864	0.36667	0.016*
N22	0.59926 (13)	0.82859 (13)	0.39284 (10)	0.01293 (14)
C23	0.51841 (17)	0.72996 (17)	0.21469 (12)	0.01786 (18)
H23A	0.580724	0.81486	0.153155	0.027*
H23B	0.380672	0.699047	0.18678	0.027*
H23C	0.539512	0.609696	0.184401	0.027*
C3	0.98700 (15)	1.25492 (15)	0.69291 (13)	0.01513 (17)
H3	1.047781	1.324625	0.625083	0.018*
C4	1.05621 (15)	1.32381 (15)	0.86576 (14)	0.01670 (18)
H4	1.166445	1.441282	0.917816	0.02*
C5	0.96252 (15)	1.21913 (15)	0.96081 (13)	0.01547 (17)
H5	1.008301	1.263236	1.078576	0.019*
C6	0.79997 (14)	1.04805 (14)	0.88085 (12)	0.01344 (16)
H6	0.734271	0.977774	0.946118	0.016*

Atomic displacement parameters (\AA^2)

	U^{11}	U^{22}	U^{33}	U^{12}	U^{13}	U^{23}
Cu1	0.01109 (6)	0.00923 (6)	0.00822 (5)	0.00253 (4)	0.00183 (4)	0.00182 (4)
Cl1	0.01209 (9)	0.01174 (9)	0.01270 (9)	0.00393 (7)	-0.00076 (7)	0.00086 (7)
Cl2	0.01607 (10)	0.01358 (10)	0.01276 (9)	0.00224 (8)	0.00631 (8)	0.00342 (7)
N1	0.0127 (3)	0.0098 (3)	0.0105 (3)	0.0037 (3)	0.0030 (3)	0.0034 (2)
C2	0.0132 (4)	0.0110 (4)	0.0128 (4)	0.0046 (3)	0.0050 (3)	0.0049 (3)
C21	0.0170 (4)	0.0150 (4)	0.0125 (4)	0.0082 (3)	0.0061 (3)	0.0065 (3)
N22	0.0162 (4)	0.0142 (4)	0.0094 (3)	0.0075 (3)	0.0029 (3)	0.0037 (3)
C23	0.0238 (5)	0.0209 (5)	0.0087 (4)	0.0100 (4)	0.0027 (3)	0.0037 (3)
C3	0.0143 (4)	0.0118 (4)	0.0188 (4)	0.0034 (3)	0.0063 (3)	0.0052 (3)

C4	0.0136 (4)	0.0119 (4)	0.0200 (4)	0.0021 (3)	0.0033 (3)	0.0020 (3)
C5	0.0149 (4)	0.0130 (4)	0.0135 (4)	0.0032 (3)	0.0008 (3)	0.0009 (3)
C6	0.0148 (4)	0.0120 (4)	0.0102 (3)	0.0029 (3)	0.0015 (3)	0.0024 (3)

Geometric parameters (Å, °)

Cu1—N1	2.0241 (9)	N22—C23	1.4580 (13)
Cu1—N22	2.0374 (8)	C23—H23A	0.98
Cu1—Cl2	2.2500 (3)	C23—H23B	0.98
Cu1—Cl1 ⁱ	2.2835 (3)	C23—H23C	0.98
Cu1—Cl1	2.6112 (3)	C3—C4	1.3953 (15)
N1—C6	1.3320 (12)	C3—H3	0.95
N1—C2	1.3561 (12)	C4—C5	1.3867 (15)
C2—C3	1.3842 (14)	C4—H4	0.95
C2—C21	1.4663 (14)	C5—C6	1.3953 (14)
C21—N22	1.2796 (13)	C5—H5	0.95
C21—H21	0.95	C6—H6	0.95
N1—Cu1—N22	80.20 (3)	C21—N22—Cu1	114.21 (7)
N1—Cu1—Cl2	92.29 (2)	C23—N22—Cu1	126.45 (7)
N22—Cu1—Cl2	155.16 (3)	N22—C23—H23A	109.5
N1—Cu1—Cl1 ⁱ	173.79 (2)	N22—C23—H23B	109.5
N22—Cu1—Cl1 ⁱ	93.61 (3)	H23A—C23—H23B	109.5
Cl2—Cu1—Cl1 ⁱ	93.600 (11)	N22—C23—H23C	109.5
N1—Cu1—Cl1	88.81 (3)	H23A—C23—H23C	109.5
N22—Cu1—Cl1	94.79 (3)	H23B—C23—H23C	109.5
Cl2—Cu1—Cl1	108.803 (10)	C2—C3—C4	118.02 (9)
Cl1 ⁱ —Cu1—Cl1	91.137 (10)	C2—C3—H3	121
Cu1 ⁱ —Cl1—Cu1	88.864 (11)	C4—C3—H3	121
C6—N1—C2	118.79 (8)	C5—C4—C3	119.36 (9)
C6—N1—Cu1	127.36 (7)	C5—C4—H4	120.3
C2—N1—Cu1	113.81 (6)	C3—C4—H4	120.3
N1—C2—C3	122.78 (9)	C4—C5—C6	118.99 (10)
N1—C2—C21	113.95 (8)	C4—C5—H5	120.5
C3—C2—C21	123.26 (9)	C6—C5—H5	120.5
N22—C21—C2	117.82 (8)	N1—C6—C5	122.05 (9)
N22—C21—H21	121.1	N1—C6—H6	119
C2—C21—H21	121.1	C5—C6—H6	119
C21—N22—C23	119.31 (9)		
C6—N1—C2—C3	-0.69 (15)	N1—C2—C3—C4	1.35 (16)
Cu1—N1—C2—C3	-178.63 (8)	C21—C2—C3—C4	-177.87 (10)
C6—N1—C2—C21	178.59 (9)	C2—C3—C4—C5	-0.67 (16)
Cu1—N1—C2—C21	0.66 (11)	C3—C4—C5—C6	-0.57 (17)
N1—C2—C21—N22	-0.97 (14)	C2—N1—C6—C5	-0.66 (15)
C3—C2—C21—N22	178.31 (10)	Cu1—N1—C6—C5	176.97 (8)

C2—C21—N22—C23	-177.41 (9)	C4—C5—C6—N1	1.29 (17)
C2—C21—N22—Cu1	0.77 (12)		

Symmetry code: (i) $-x+1, -y+1, -z+1$.

Hydrogen-bond geometry (Å, °)

<i>D—H...A</i>	<i>D—H</i>	<i>H...A</i>	<i>D...A</i>	<i>D—H...A</i>
C6—H6...Cl2	0.95	2.71	3.2301 (10)	115
